Systematic investigation of changes in oxidized cerebral cytochrome *c* oxidase concentration during frontal lobe activation in healthy adults

Christina Kolyva,[1,*] Ilias Tachtsidis,[1] Arnab Ghosh,[2] Tracy Moroz,[1] Chris E. Cooper,[3] Martin Smith,[1,2] and Clare E. Elwell[1]

[1]Medical Physics & Bioengineering, University College London, London WC1E 6BT, UK
[2]Neurocritical Care Unit, University College London Hospitals, London WC1N 3BG, UK
[3]Biological Sciences, University of Essex, Colchester CO4 3SQ, UK
*c.kolyva@ucl.ac.uk

Abstract: Using transcranial near-infrared spectroscopy (NIRS) to measure changes in the redox state of cerebral cytochrome *c* oxidase (Δ[oxCCO]) during functional activation in healthy adults is hampered by instrumentation and algorithm issues. This study reports the Δ[oxCCO] response measured in such a setting and investigates possible confounders of this measurement. Continuous frontal lobe NIRS measurements were collected from 11 healthy volunteers during a 6-minute anagram-solving task, using a hybrid optical spectrometer (pHOS) that combines multi-distance frequency and broadband components. Only data sets showing a hemodynamic response consistent with functional activation were interrogated for a Δ[oxCCO] response. Simultaneous systemic monitoring data were also available. Possible influences on the Δ[oxCCO] response were systematically investigated and there was no effect of: 1) wavelength range chosen for fitting the measured attenuation spectra; 2) constant or measured, with the pHOS in real-time, differential pathlength factor; 3) systemic hemodynamic changes during functional activation; 4) changes in optical scattering during functional activation. The Δ[oxCCO] response measured in the presence of functional activation was heterogeneous, with the majority of subjects showing significant increase in oxidation, but others having a decrease. We conclude that the heterogeneity in the Δ[oxCCO] response is physiological and not induced by confounding factors in the measurements.

© 2012 Optical Society of America

OCIS codes: (170.0170) Medical optics and biotechnology; (170.6510) Spectroscopy, tissue diagnostics; (170.2655) Functional monitoring and imaging; (170.1610) Clinical applications; (170.5380) Physiology; (300.6190) Spectrometers.

References and links

1. H. Obrig and A. Villringer, "Beyond the visible--imaging the human brain with light," J. Cereb. Blood Flow Metab. **23**(1), 1–18 (2003).
2. Y. Kakihana, A. Matsunaga, T. Yasuda, T. Imabayashi, Y. Kanmura, and M. Tamura, "Brain oxymetry in the operating room: current status and future directions with particular regard to cytochrome oxidase," J. Biomed. Opt. **13**(3), 033001 (2008).
3. D. Highton, C. Elwell, and M. Smith, "Noninvasive cerebral oximetry: is there light at the end of the tunnel?" Curr. Opin. Anaesthesiol. **23**(5), 576–581 (2010).
4. M. Wolf, M. Ferrari, and V. Quaresima, "Progress of near-infrared spectroscopy and topography for brain and muscle clinical applications," J. Biomed. Opt. **12**(6), 062104 (2007).
5. C. E. Cooper, M. Cope, R. Springett, P. N. Amess, J. Penrice, L. Tyszczuk, S. Punwani, R. Ordidge, J. Wyatt, and D. T. Delpy, "Use of mitochondrial inhibitors to demonstrate that cytochrome oxidase near-infrared spectroscopy can measure mitochondrial dysfunction noninvasively in the brain," J. Cereb. Blood Flow Metab. **19**(1), 27–38 (1999).

6. C. E. Cooper and R. Springett, "Measurement of cytochrome oxidase and mitochondrial energetics by near-infrared spectroscopy," Philos. Trans. R. Soc. Lond. B Biol. Sci. **352**(1354), 669–676 (1997).
7. F. F. Jöbsis, "Noninvasive, infrared monitoring of cerebral and myocardial oxygen sufficiency and circulatory parameters," Science **198**(4323), 1264–1267 (1977).
8. M. Banaji, "A generic model of electron transport in mitochondria," J. Theor. Biol. **243**(4), 501–516 (2006).
9. M. Banaji, A. Mallet, C. E. Elwell, P. Nicholls, and C. E. Cooper, "A model of brain circulation and metabolism: NIRS signal changes during physiological challenges," PLOS Comput. Biol. **4**(11), e1000212 (2008).
10. M. M. Tisdall, I. Tachtsidis, T. S. Leung, C. E. Elwell, and M. Smith, "Changes in the attenuation of near infrared spectra by the healthy adult brain during hypoxaemia cannot be accounted for solely by changes in the concentrations of oxy- and deoxy-haemoglobin," Adv. Exp. Med. Biol. **614**, 217–225 (2008).
11. K. Uludag, M. Kohl, J. Steinbrink, H. Obrig, and A. Villringer, "Cross talk in the Lambert-Beer calculation for near-infrared wavelengths estimated by Monte Carlo simulations," J. Biomed. Opt. **7**(1), 51–59 (2002).
12. K. Uludağ, J. Steinbrink, M. Kohl-Bareis, R. Wenzel, A. Villringer, and H. Obrig, "Cytochrome-c-oxidase redox changes during visual stimulation measured by near-infrared spectroscopy cannot be explained by a mere cross talk artefact," Neuroimage **22**(1), 109–119 (2004).
13. R. Springett, J. Newman, M. Cope, and D. T. Delpy, "Oxygen dependency and precision of cytochrome oxidase signal from full spectral NIRS of the piglet brain," Am. J. Physiol. Heart Circ. Physiol. **279**(5), H2202–H2209 (2000).
14. H. R. Heekeren, M. Kohl, H. Obrig, R. Wenzel, W. von Pannwitz, S. J. Matcher, U. Dirnagl, C. E. Cooper, and A. Villringer, "Noninvasive assessment of changes in cytochrome-c oxidase oxidation in human subjects during visual stimulation," J. Cereb. Blood Flow Metab. **19**(6), 592–603 (1999).
15. M. M. Tisdall, I. Tachtsidis, T. S. Leung, C. E. Elwell, and M. Smith, "Increase in cerebral aerobic metabolism by normobaric hyperoxia after traumatic brain injury," J. Neurosurg. **109**(3), 424–432 (2008).
16. M. M. Tisdall, I. Tachtsidis, T. S. Leung, C. E. Elwell, and M. Smith, "Near-infrared spectroscopic quantification of changes in the concentration of oxidized cytochrome c oxidase in the healthy human brain during hypoxemia," J. Biomed. Opt. **12**(2), 024002 (2007).
17. I. Tachtsidis, M. M. Tisdall, T. S. Leung, C. Pritchard, C. E. Cooper, M. Smith, and C. E. Elwell, "Relationship between brain tissue haemodynamics, oxygenation and metabolism in the healthy human adult brain during hyperoxia and hypercapnea," Adv. Exp. Med. Biol. **645**, 315–320 (2009).
18. I. Tachtsidis, M. Tisdall, T. S. Leung, C. E. Cooper, D. T. Delpy, M. Smith, and C. E. Elwell, "Investigation of in vivo measurement of cerebral cytochrome-c-oxidase redox changes using near-infrared spectroscopy in patients with orthostatic hypotension," Physiol. Meas. **28**(2), 199–211 (2007).
19. Y. Kakihana, A. Matsunaga, K. Tobo, S. Isowaki, M. Kawakami, I. Tsuneyoshi, Y. Kanmura, and M. Tamura, "Redox behavior of cytochrome oxidase and neurological prognosis in 66 patients who underwent thoracic aortic surgery," Eur. J. Cardiothorac. Surg. **21**(3), 434–439 (2002).
20. A. D. McGown, H. Makker, C. Elwell, P. G. Al Rawi, A. Valipour, and S. G. Spiro, "Measurement of changes in cytochrome oxidase redox state during obstructive sleep apnea using near-infrared spectroscopy," Sleep **26**(6), 710–716 (2003).
21. I. Tachtsidis, L. Gao, T. S. Leung, M. Kohl-Bareis, C. E. Cooper, and C. E. Elwell, "A hybrid multi-distance phase and broadband spatially resolved spectrometer and algorithm for resolving absolute concentrations of chromophores in the near-infrared light spectrum," Adv. Exp. Med. Biol. **662**, 169–175 (2010).
22. L. Aziz-Zadeh, J. T. Kaplan, and M. Iacoboni, "'Aha!': The neural correlates of verbal insight solutions," Hum. Brain Mapp. **30**(3), 908–916 (2009).
23. N. M. Gregg, B. R. White, B. W. Zeff, A. J. Berger, and J. P. Culver, "Brain specificity of diffuse optical imaging: improvements from superficial signal regression and tomography," Front Neuroenergetics **2**, 14 (2010).
24. I. Tachtsidis, T. S. Leung, A. Chopra, P. H. Koh, C. B. Reid, and C. E. Elwell, "False positives in functional near-infrared topography," Adv. Exp. Med. Biol. **645**, 307–314 (2009).
25. L. Minati, I. U. Kress, E. Visani, N. Medford, and H. D. Critchley, "Intra- and extra-cranial effects of transient blood pressure changes on brain near-infrared spectroscopy (NIRS) measurements," J. Neurosci. Methods **197**(2), 283–288 (2011).
26. T. Takahashi, Y. Takikawa, R. Kawagoe, S. Shibuya, T. Iwano, and S. Kitazawa, "Influence of skin blood flow on near-infrared spectroscopy signals measured on the forehead during a verbal fluency task," Neuroimage **57**(3), 991–1002 (2011).
27. I. Tachtsidis, T. S. Leung, L. Devoto, D. T. Delpy, and C. E. Elwell, "Measurement of frontal lobe functional activation and related systemic effects: a near-infrared spectroscopy investigation," Adv. Exp. Med. Biol. **614**, 397–403 (2008).
28. I. Tachtsidis, T. S. Leung, M. M. Tisdall, P. Devendra, M. Smith, D. T. Delpy, and C. E. Elwell, "Investigation of frontal cortex, motor cortex and systemic haemodynamic changes during anagram solving," Adv. Exp. Med. Biol. **614**, 21–28 (2008).
29. I. Tachtsidis, T. S. Leung, B. Tahir, C. E. Elwell, M. Kohl-Bareis, M. Gramer, and C. E. Cooper, "A hybrid multi-distance phase and broadband spatially resolved algorithm for resolving absolute concentrations of chromophores in the near-infrared light spectrum: application on to dynamic phantoms," in *Biomedical Optics*, OSA Technical Digest (Optical Society of America, 2008), paper BSuE76.

30. L. Gao, C. E. Elwell, M. Kohl-Bareis, M. Gramer, C. E. Cooper, T. S. Leung, and I. Tachtsidis, "Effects of assuming constant optical scattering on haemoglobin concentration measurements using NIRS during a Valsalva manoeuvre," Adv. Exp. Med. Biol. **701**, 15–20 (2011).
31. S. Fantini, D. Hueber, M. A. Franceschini, E. Gratton, W. Rosenfeld, P. G. Stubblefield, D. Maulik, and M. R. Stankovic, "Non-invasive optical monitoring of the newborn piglet brain using continuous-wave and frequency-domain spectroscopy," Phys. Med. Biol. **44**(6), 1543–1563 (1999).
32. E. R. Reilly, "EEG recording and operation of the apparatus," in *Electroencephalography: Basic Principles, Clinical Applications and Related Fields,* E. Niedermeyer and F. H. L. Da Silva, eds. (Lippincott Williams and Wilkins, 2005), pp. 139–160.
33. S. J. Matcher, C. E. Elwell, C. E. Cooper, M. Cope, and D. T. Delpy, "Performance comparison of several published tissue near-infrared spectroscopy algorithms," Anal. Biochem. **227**(1), 54–68 (1995).
34. M. Essenpreis, C. E. Elwell, M. Cope, P. van der Zee, S. R. Arridge, and D. T. Delpy, "Spectral dependence of temporal point spread functions in human tissues," Appl. Opt. **32**(4), 418–425 (1993).
35. A. Duncan, J. H. Meek, M. Clemence, C. E. Elwell, L. Tyszczuk, M. Cope, and D. T. Delpy, "Optical pathlength measurements on adult head, calf and forearm and the head of the newborn infant using phase resolved optical spectroscopy," Phys. Med. Biol. **40**(2), 295–304 (1995).
36. C. E. Cooper, S. J. Matcher, J. S. Wyatt, M. Cope, G. C. Brown, E. M. Nemoto, and D. T. Delpy, "Near-infrared spectroscopy of the brain: relevance to cytochrome oxidase bioenergetics," Biochem. Soc. Trans. **22**(4), 974–980 (1994).
37. B. Chance and G. R. Williams, "Respiratory enzymes in oxidative phosphorylation. III. The steady state," J. Biol. Chem. **217**(1), 409–427 (1955).
38. C. W. Shuttleworth, A. M. Brennan, and J. A. Connor, "NAD(P)H fluorescence imaging of postsynaptic neuronal activation in murine hippocampal slices," J. Neurosci. **23**(8), 3196–3208 (2003).
39. M. A. Mintun, B. N. Lundstrom, A. Z. Snyder, A. G. Vlassenko, G. L. Shulman, and M. E. Raichle, "Blood flow and oxygen delivery to human brain during functional activity: theoretical modeling and experimental data," Proc. Natl. Acad. Sci. U.S.A. **98**(12), 6859–6864 (2001).
40. S. Asgari, A. Doerfler, T. Engelhorn, H. J. Röhrborn, and D. Stolke, "In-vivo measurement of cytochrome using NIRS during acute focal cerebral ischaemia and reperfusion in rats," Zentralbl. Neurochir. **63**(04), 146–152 (2002).
41. F. Orihuela-Espina, D. R. Leff, D. R. James, A. W. Darzi, and G. Z. Yang, "Quality control and assurance in functional near infrared spectroscopy (fNIRS) experimentation," Phys. Med. Biol. **55**(13), 3701–3724 (2010).
42. F. Tian, B. Chance, and H. Liu, "Investigation of the prefrontal cortex in response to duration-variable anagram tasks using functional near-infrared spectroscopy," J. Biomed. Opt. **14**(5), 054016 (2009).
43. F. Schneider, R. E. Gur, A. Alavi, M. E. Seligman, L. H. Mozley, R. J. Smith, P. D. Mozley, and R. C. Gur, "Cerebral blood flow changes in limbic regions induced by unsolvable anagram tasks," Am. J. Psychiatry **153**(2), 206–212 (1996).
44. O. Vartanian and V. Goel, "Task constraints modulate activation in right ventral lateral prefrontal cortex," Neuroimage **27**(4), 927–933 (2005).
45. D. L. Drabkin, "Metabolism of the hemin chromoproteins," Physiol. Rev. **31**(4), 345–431 (1951).
46. M. Smith and C. Elwell, "Near-infrared spectroscopy: shedding light on the injured brain," Anesth. Analg. **108**(4), 1055–1057 (2009).
47. H. W. Schytz, T. Wienecke, L. T. Jensen, J. Selb, D. A. Boas, and M. Ashina, "Changes in cerebral blood flow after acetazolamide: an experimental study comparing near-infrared spectroscopy and SPECT," Eur. J. Neurol. **16**(4), 461–467 (2009).
48. T. J. Germon, P. D. Evans, N. J. Barnett, P. Wall, A. R. Manara, and R. J. Nelson, "Cerebral near infrared spectroscopy: emitter-detector separation must be increased," Br. J. Anaesth. **82**(6), 831–837 (1999).
49. T. J. Germon, P. D. Evans, A. R. Manara, N. J. Barnett, P. Wall, and R. J. Nelson, "Sensitivity of near infrared spectroscopy to cerebral and extra-cerebral oxygenation changes is determined by emitter-detector separation," J. Clin. Monit. Comput. **14**(5), 353–360 (1998).
50. M. Dehaes, P. E. Grant, D. D. Sliva, N. Roche-Labarbe, R. Pienaar, D. A. Boas, M. A. Franceschini, and J. Selb, "Assessment of the frequency-domain multi-distance method to evaluate the brain optical properties: Monte Carlo simulations from neonate to adult," Biomed. Opt. Express **2**(3), 552–567 (2011).
51. T. Correia, A. Gibson, and J. Hebden, "Identification of the optimal wavelengths for optical topography: a photon measurement density function analysis," J. Biomed. Opt. **15**(5), 056002 (2010).

1. Introduction

Near-infrared spectroscopy (NIRS) is a widely used optical method of monitoring, non-invasively and with good time resolution, regional changes in chromophore concentration in various types of biological tissue, including the adult brain [1–4]. NIRS can provide information not only about cerebral oxygen delivery, via measured concentration changes of oxygenated ($\Delta[HbO_2]$) and deoxygenated haemoglobin ($\Delta[HHb]$), but, with suitable instrumentation and algorithms [5,6], also about local cellular oxygen metabolism, via measuring concentration changes of oxidised cytochrome c oxidase ($\Delta[oxCCO]$).

Cytochrome *c* oxidase (CCO) is the terminal enzyme of the mitochondrial respiratory chain and catalyses over 95% of oxygen metabolism. It contains four redox-active metal centres, of which the copper A (Cu_A) centre has a distinct redox-sensitive absorbance band in the near infrared [7]. In the short term the total concentration of CCO does not change, consequently changes in the NIRS-obtained Δ[oxCCO] signal track changes in the CCO redox state. The CCO redox state is a complex function of the delivery of redox substrates (oxygen, NADH) into mitochondria and the magnitude of the mitochondrial proton electrochemical potential that drives ATP synthesis [8]. The Δ[oxCCO] signal - appropriately interpreted with the aid of mathematical modelling (BRAINSIGNALS model [9]) - can therefore be used as a non-invasive marker of changes in mitochondrial oxygen consumption and utilisation. Because of this capacity, it provides an appealing target for clinical monitoring, with the potential to aid the early detection of regional ischemia and guide subsequent therapeutic interventions.

The transcranial NIRS measurement of Δ[oxCCO] in the adult brain, in the presence of significantly higher concentrations of haemoglobin, poses certain technical challenges. Possible interference of changes in optical scattering with the NIRS measurements [5,6] and insufficient separation of the chromophores by the algorithm used to convert optical density into changes in chromophore concentration [5,6,10–13] are the most frequently mentioned confounding effects. Despite these issues, several studies have reported Δ[oxCCO] measurements in the adult brain in a variety of settings, including visual stimulation [12,14], traumatic brain injury [15], manipulation of cerebral oxygen delivery [16,17], orthostatic hypotension [18], cardiopulmonary bypass during cardiac surgery [19] and obstructive sleep apnoea [20].

A hybrid optical spectrometer (pHOS) and associated algorithm designed to address the aforementioned technical issues have been recently developed by our group [21]. The pHOS combines multi-distance frequency and broadband spectrometers, and allows for measurements of light absorption and scattering at discrete wavelengths, together with multi-distance broadband near-infrared light attenuation measurements.

Neurovascular coupling refers to the mechanism describing the tight coupling between local cerebral neuronal activity and subsequent changes in cerebral blood flow to meet local oxygen demand [1]. It is these local changes in cerebral hemodynamics and oxygenation that can be measured by NIRS. Functional activation through anagram solving induces bilateral frontal hemodynamic response detected by NIRS as an increase in HbO_2 concentration and a decrease in HHb concentration [1]. This scenario provides an excellent paradigm for an NIRS study and the activated part of the brain can be monitored with optodes placed over a hairless and easily-accessible part of the scalp. Therefore, for the purpose of monitoring Δ[oxCCO] in the healthy adult brain with NIRS in the presence of increased brain activity, anagram solving provides a convenient setting [22]. Confounding task-induced systemic changes need to be measured simultaneously since they could affect the NIRS signals [23–26].

The aim of this study was to use the pHOS to investigate the response of Δ[oxCCO] to frontal lobe functional activation in healthy adult volunteers. In order to explore this aim the objectives of this study were 1) to measure the Δ[oxCCO] response in different layers of the head using multi-distance broadband spectroscopy in the presence of a hemodynamic response consistent with frontal lobe activation and 2) to investigate systematically multiple possible confounds of these measurements.

2. Methods

2.1. Study population and protocol

Eleven healthy volunteers participated in the study (7 male; age range 21-34 years). Ten subjects were right-handed. The study was approved by the UCL Ethics Committee and written informed consent was obtained from all subjects.

All volunteers were seated in a comfortable position. An anagram exercise protocol previously described by our group was followed [27,28]. Briefly, data were continuously collected during a 2-minute baseline, followed by a sequence of 1 minute of 4-letter anagrams and 1 minute of 7-letter anagrams, each repeated three times, and concluded by another 2-minute baseline. The total duration of the recordings was therefore 10 minutes. The subjects were encouraged to solve as many anagrams as possible, without verbalising the solutions.

2.2. Instrumentation

The pHOS has been described elsewhere [21,29,30]. Briefly, it consists of a dual-channel frequency domain (FD) spectrometer and two single-channel broadband spectrometers. The FD component of the pHOS is a modified commercially available system (ISS Oximeter, model 96208, ISS Inc, Champaign, IL, USA) operating at a modulation frequency of 110 MHz. Light is emitted at wavelengths 690, 750, 790 and 850 nm and two source-detector separations (3.0 and 3.5 cm) are available. The instrument measures the mean value, amplitude and phase shift of the modulated light intensity for the two different source-detector separations at each wavelength. These measurements are subsequently used for quantifying the absorption (μ_a) and reduced scattering (μ_s') coefficients of the measured tissue [31].

Each broadband spectrometer of the pHOS utilises a 50W halogen bulb as a white light source and a filter is implemented to reduce the effect of high temperature. After passing through a configuration of lenses, the light is detected by a CCD camera (Pixis 512, Princeton Instruments, Trenton, NJ, USA) with chip dimensions 12.3x12.3 mm (512x512 pixels). Through four detector fibres with different diameters and oval cross-section, the light is directed to four detectors situated at distances 2.0, 2.5, 3.0 and 3.5 cm away from the light source. The optical bandwidth of the broadband spectrometers is 504-1068 nm with wavelength resolution of 4 nm.

Each of the two optodes of the pHOS incorporates one channel of the FD system with a broadband channel. This configuration leads to the two long source-detector separations (3.0 and 3.5 cm) being the same for each broadband and FD channel, with each broadband channel having available two additional shorter source-detector separations (2.0 and 2.5 cm). Recordings in the two pHOS channels occur in parallel, but within each channel the FD and broadband measurements are taken sequentially, with the FD system providing the trigger. Each measurement cycle consists of one broadband measurement followed by four FD measurements, resulting in a cycle length of 3.2 s.

With the ability to interrogate the same tissue segment simultaneously for μ_a and μ_s' and for broadband light attenuation data, combined with the ability to perform these measurements at multiple source-detector separations, the pHOS may provide optical data that can help resolve most of the technical issues commonly hampering Δ[oxCCO] measurements.

2.3. Measurements

All pHOS measurements were obtained unilaterally on the right side of the forehead throughout the protocol, with optodes placed over the Fp2, according to the 10-20 system of electrode placement [32]. Simultaneously, arterial blood pressure (BP) and heart rate (HR) were measured with a Portapres® system (Finapres Medical Systems, The Netherlands). Scalp blood flow (LD Flux) was also monitored with a laser Doppler probe placed on the forehead (Moor Instruments, UK).

2.4. Data analysis

All data analysis was performed in Matlab (version R2010b, Mathworks, Natick, MA, USA).

The modified Beer-Lambert law was used to determine changes in Δ[HbO$_2$], Δ[HHb] and Δ[oxCCO], based on measured changes in broadband near-infrared light attenuation. The concentration calculations were undertaken for each of the four single source-detector combinations throughout rest, anagram exercise and recovery continuously. A least-squares

fitting procedure (UCLn algorithm [33]) was implemented for these calculations over two different wavelength ranges, 740-900 nm and 780-900 nm. The UCLn algorithm is based on multiple linear regression analysis, utilising the Beer-Lambert law to determine the best fit of the chromophore specific extinction coefficients, ε, to the measured attenuation changes, ΔA, over n number of wavelengths, λ:

$$
\begin{bmatrix} \Delta[HbO_2] \\ \Delta[HHb] \\ \Delta[oxCCO] \end{bmatrix} = \frac{1}{pathlengh} \begin{bmatrix} \varepsilon_{HbO_2}(\lambda_1) & \varepsilon_{HHb}(\lambda_1) & \varepsilon_{oxCCO}(\lambda_1) \\ \varepsilon_{HbO_2}(\lambda_2) & \varepsilon_{HHb}(\lambda_2) & \varepsilon_{oxCCO}(\lambda_2) \\ ... & ... & ... \\ \varepsilon_{HbO_2}(\lambda_n) & \varepsilon_{HHb}(\lambda_n) & \varepsilon_{oxCCO}(\lambda_n) \end{bmatrix}^{-1} \begin{bmatrix} \Delta A(\lambda_1) \\ \Delta A(\lambda_2) \\ ... \\ \Delta A(\lambda_n) \end{bmatrix} \quad (1)
$$

The specific extinction coefficient spectra used to resolve $\Delta[HbO_2]$, $\Delta[HHb]$ and $\Delta[oxCCO]$ are provided as online supplementary material (see Media 1).

Differential pathlength factor (DPF) falls with increasing wavelength and this wavelength dependence was taken into account in all four broadband detectors [34]. DPF was assumed to be constant and equal to 6.26 for the two broadband detectors proximal to the light source [35]. At the location of the two distal detectors, time-varying DPF was derived from the FD measurements using the μ_a and μ_s' measured at 690, 750, 790 and 850 nm [31]. From these DPF calculations, the time-varying DPF measured at 790 nm was used for the concentration calculations of the two distal broadband detectors. For these detectors the concentration calculations were repeated assuming DPF constant and equal to the first baseline value of the aforementioned time-varying DPF series.

The calculated chromophore concentration changes, together with the μ_a, μ_s', DPF and the systemic data were resampled every 3s and the derived concentration data were linearly detrended to remove possible baseline drifts. Subsequently all data were processed with a low-pass 5th order Butterworth filter with a cut-off frequency of 0.08Hz.

There was a total of 4 data sets for analysis from each subject, corresponding to four source-detector separations. To select representative data during baseline and activation, suitable baseline and activation periods had to be determined for data averaging. The activation period for $\Delta[HbO_2]$ was defined as the 60-second window of max $\Delta[HbO_2]$ increase with respect to baseline. The $\Delta[HHb]$ and $\Delta[oxCCO]$ traces were subsequently scanned separately for the 60-second window of maximum change with respect to baseline. The search areas for these windows were tied to the $\Delta[HbO_2]$ activation window, with the windows allowed to start as early as 57 s prior the start of the $\Delta[HbO_2]$ window and end as late as 57 s after the end of the $\Delta[HbO_2]$ window (Fig. 1). All activation windows were set to remain entirely inside the anagram exercise period, by not allowing the windows to start prior to the onset of the exercise and end after the finish of the exercise (Fig. 1). Averages for the systemic and scattering data during activation were also calculated inside the CCO activation window. The baseline period was defined for all parameters as the 60-second window immediately prior to the onset of the anagram exercise. For all parameters "response" is defined as the difference between activation and baseline.

In order to ensure that only $\Delta[oxCCO]$ traces concomitant with increased brain activity were interrogated, only subjects showing hemodynamic response consistent with functional activation (a statistically significant increase in $\Delta[HbO_2]$ and a simultaneous, statistically significant decrease or no response of $\Delta[HHb]$ [1]) were entered into the analysis described in this study.

The UCLn algorithm was also used to derive changes in chromophore concentrations when resolving for 2 chromophores only (HbO_2 and HHb) [33]. Attenuation-change spectra (change in attenuation over the wavelength range resolved) for both 2- and 3-chromophore fits were back-calculated from the concentration changes derived from the UCLn algorithm (prior
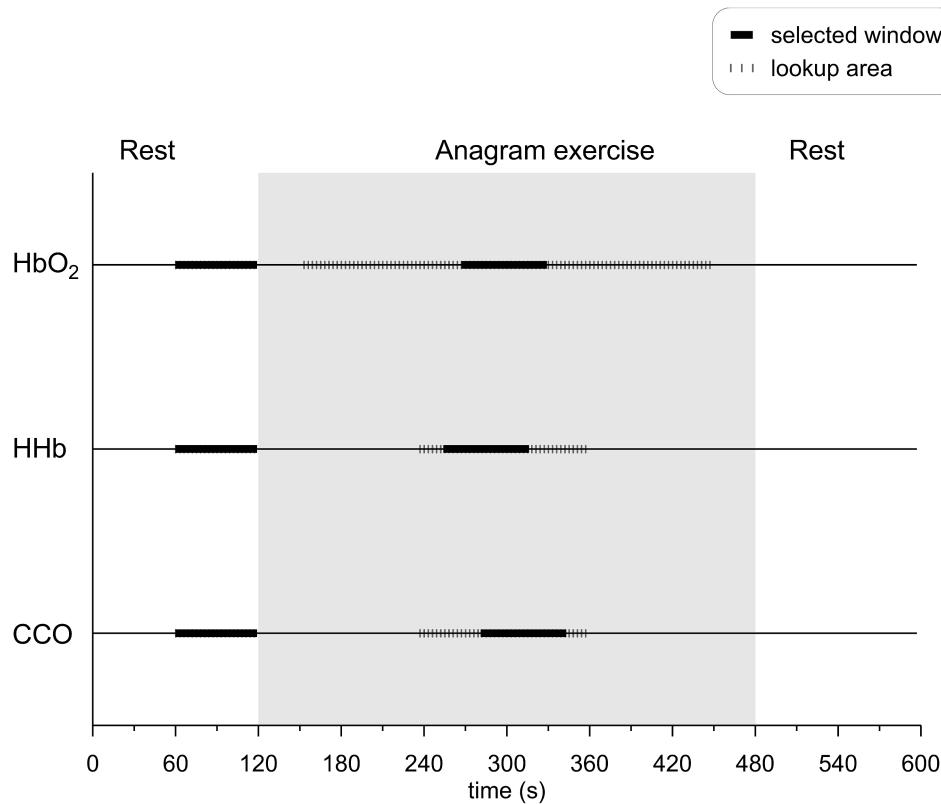
Fig. 1. Selection of baseline and activation time windows for the three chromophores. For all chromophores the baseline window was the 60-second window just before the subject started solving anagrams. The activation window for HbO_2 was the 60-second window of maximum $\Delta[HbO_2]$ increase with respect to baseline. The search area for the middle of this window was any time during the anagram exercise, except for the first and last 30 seconds. The activation windows for CCO and HHb were the 60-second windows of maximum $\Delta[HHb]$ and $\Delta[oxCCO]$ response with respect to baseline. The search areas for the centres of both windows were tied to the HbO_2 activation window and were set to start as early as 27 seconds before the beginning of the HbO_2 window and end as late as 27 seconds after its end.

to detrending or filtering), at all sampling points falling within the activation window of $\Delta[oxCCO]$.

2.5. Statistical analysis

All statistical analysis was carried out in SPSS (v 18.0, IBM, NY, USA). Student's unpaired t-tests were used to compare, for all parameters, the means of the selected baseline and activation points. Responses between the four detectors were compared using analysis of variance with repeated measures followed by contrast analysis. Linear regression analysis was performed separately for each detector to investigate, over all subjects, possible relations between various parameters. Average data are expressed as mean $\pm$ SD and statistical significance was set to $p < 0.05$.

3. Results

3.1. Hemodynamic response and choice of channels

Out of 11 subjects, 8 showed hemodynamic response consistent with functional activation (as defined in the Methods section) and within each subject there was excellent agreement
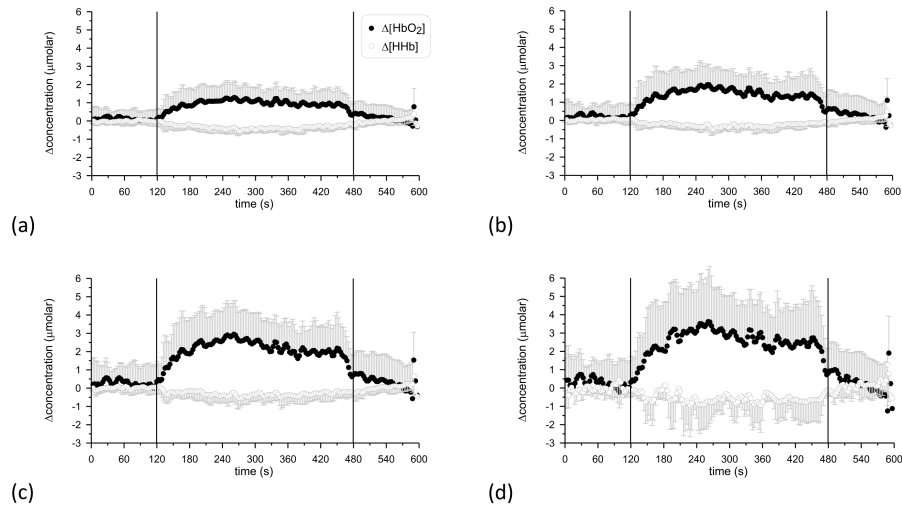
Fig. 2. Grand averages of the time course of $\Delta[HbO_2]$ and $\Delta[HHb]$ over the 8 subjects that showed hemodynamic response consistent with functional activation. The vertical lines at 120 s and 480 s denote the onset and end of anagram exercise. (a): detector 1 (furthest detector); (b): detector 2; (c): detector 3; (d): detector 4.

between the 4 detectors. Only 1 of the 8 subjects showed a discrepancy between detectors, in the directional changes in HbO_2 and HHb. Figure 2 shows the grand average of the $\Delta[HbO_2]$ and $\Delta[HHb]$ time courses over these 8 subjects for all detectors.

Systemic data were not available for 1 out of 8 subjects.

3.2. Multi-distance response of Δ[HbO₂]

Figure 3 shows separately for each detector the $\Delta[HbO_2]$ response to functional activation from each subject. On average, the $\Delta[HbO_2]$ response over all 8 subjects that showed hemodynamic response was 1.2 ± 1.0 µmolar (detector 1), 1.8 ± 1.2 µmolar (detector 2), 2.3 ± 1.4 µmolar (detector 3) and 2.8 ± 2.1 µmolar (detector 4), from the detector furthest to the detector nearest to the source. Within each subject the response tended to be smaller for larger
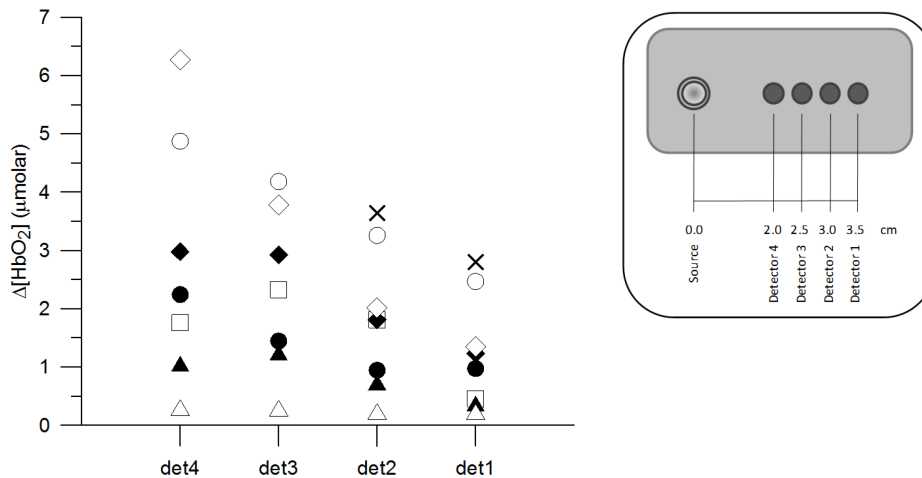

Fig. 3. Response of $\Delta[HbO_2]$ between baseline and activation for each of the four detectors. Each symbol corresponds to a different subject, in agreement with Fig. 4, 5 and 6. det1-4 denotes detector number, as indicated in the legend. No hemodynamic response consistent with functional activation was recorded in detectors 3 and 4 for subject "X".

source-detector separations and on average it was statistically significantly different between detectors 1-2 and 2-3, but not between 3 and 4. The average time to-peak-response from the onset of anagram exercise was 153.3 ± 35.2 s, 138.7 ± 26.2 s, 138.8 ± 24.9 s and 144.8 ± 34.1 s, from the distal to the proximal detector with no statistically significant difference between detectors.

3.3. Possible influencing factors on the $\Delta[oxCCO]$ measurements

Potential influencing factors on the $\Delta[oxCCO]$ measurements were explored on the data from the furthest detector, unless explicitly stated otherwise. This choice was driven by the fact that measurements from the furthest detector are more likely to reflect cerebral changes.

3.3.1. Wavelength range

For the furthest detector, the overall averages of the time courses of $\Delta[HbO_2]$, $\Delta[HHb]$ and $\Delta[oxCCO]$ in all 8 subjects were calculated twice, once for wavelength range 740-900 nm and once for 780-900 nm. Comparison for each chromophore of the average time course for the two wavelength ranges, suggested no effect of the selected wavelength range on the calculation of the concentration changes . Based on these results and in accordance with previously published data from our group, only results from the 780-900 nm wavelength range are discussed throughout this study, unless explicitly stated otherwise [10,15,16].

3.3.2. Analysis of the 2- and 3-chromophore fit spectra

The back-calculated attenuation-change spectra from the furthest detector are shown in Fig. 4 as the difference between the 3 and the 2-chromophore fit for the 8 subjects showing the required hemodynamic response. It is noted that the spectrum presented for each subject is an average spectrum, derived from all individual spectra corresponding to the 60-second $\Delta[oxCCO]$ peak activation window. The spectra do not have an arbitrary distribution around y = 0, but appear to show a shape approximating the oxidised minus reduced CCO spectrum, featuring a broad peak at approximately 820 nm. This suggests that fitting the measured changes in near-infrared attenuation only for HHb and HbO_2 would leave a chromophore with the spectral features of CCO unaccounted for.

Based on these findings only results from the 3-chromophre fit are discussed throughout this study, unless explicitly stated otherwise.

3.3.3. Pathlength

For the two furthest detectors, using a time-variant DPF or a constant DPF made no statistically significant difference in the individual time traces of $\Delta[HbO_2]$, $\Delta[HHb]$ and $\Delta[oxCCO]$ in any subject, neither in terms of amplitude of response nor in terms of time to-peak-response (data not shown). Based on these findings all results discussed throughout this study for the two furthest detectors are for time-varying DPF, unless explicitly stated otherwise.

The pathlengths used for the concentration calculations in each detector are given in Table 1. For the two furthest detectors where time-varying DPF was used, on average over the 8 subjects there was no statistically significant difference between the baseline and activation DPF value used for the concentration calculations.

Time-variant DPF derived from the FD measurements was used for the two detectors furthest away from the source (1 and 2). Mean pathlength values corresponding to the baseline and CCO activation windows are presented in the table. For detectors 3 and 4 constant DPF was used.
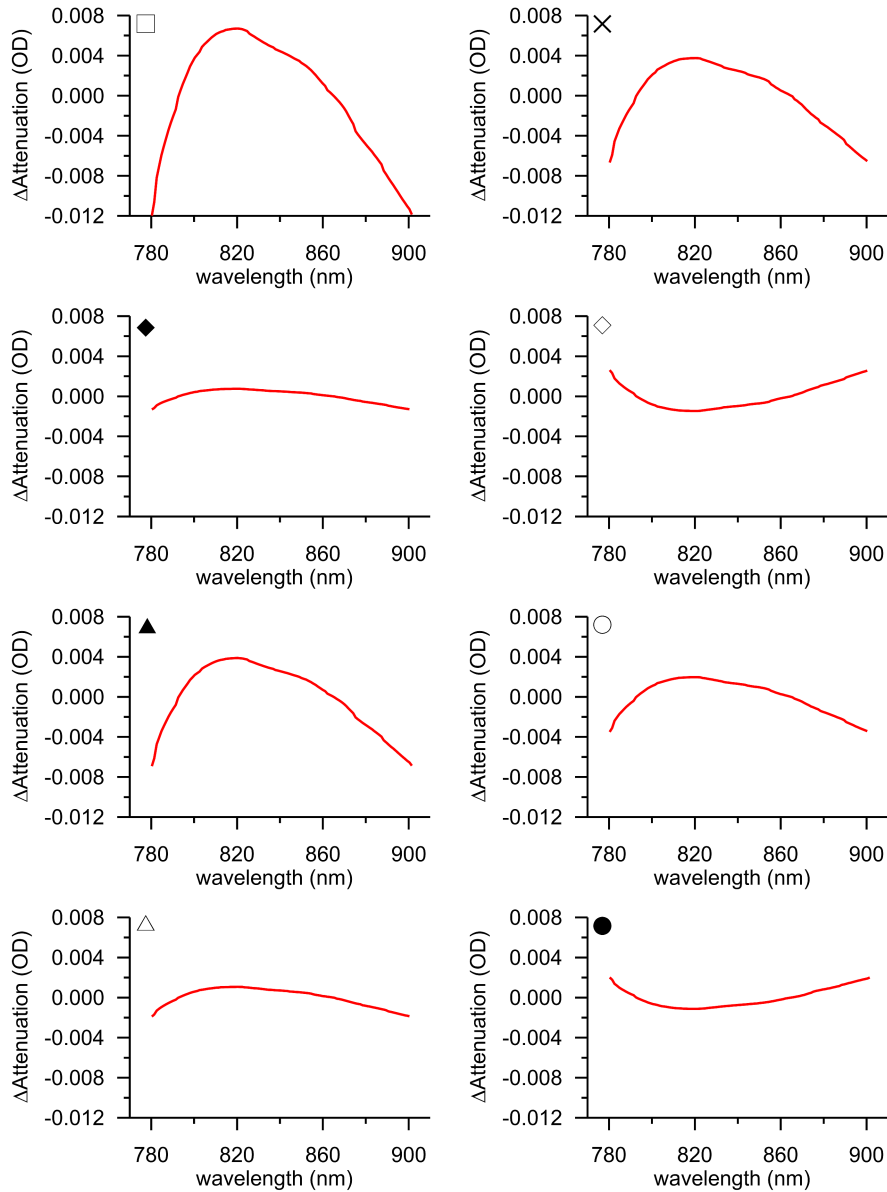
Fig. 4. Attenuation-change spectra back-calculated from the calculated concentration changes at peak Δ[oxCCO] response for different subjects. The presented spectra are the average of all spectra falling within the window of peak Δ[oxCCO] activation. The difference between the 3 and the 2-chromophore fit is plotted. All data are from the furthest detector. The symbols at the top left-hand-side corner of each plot indicate the correspondence with Fig. 3, 5 and 6.

Table 1. Pathlength, presented as DPF x distance (group data, n = 8)

Detector 1		Detector 2		Detector 3	Detector 4
Baseline	*In CCO activation window*	*Baseline*	*In CCO activation window*		
(8.0 ± 0.5) x3.5 cm	(8.1 ± 0.5) x3.5 cm	(8.0 ± 0.5) x3.0 cm	(8.1 ± 0.5) x3.0 cm	6.26 x2.5 cm	6.26 x2.0 cm

3.3.4. Concomitant systemic hemodynamic changes

A potential confounding effect of task-induced systemic changes on the Δ[oxCCO] response was explored by investigating possible associations between the amplitude of Δ[oxCCO] response with the corresponding changes in BP, HR and LD Flux calculated within the same baseline and activation windows as Δ[oxCCO]. No significant correlation was found with any systemic parameters in any detector, with a mean correlation coefficient of $R = 0.5$ for BP, $R = 0.30$ for LD Flux and $R = 0.20$ for HR.

3.3.5. Concomitant changes in optical scattering

The response of Δ[oxCCO] to functional activation was not statistically significantly related to the corresponding response of μ_s' in any detector, neither at 790 nm nor at 850 nm (data not shown). Linear regression analysis revealed no statistically significant correlations, with an average R-value over all detectors of $R = 0.28$ for 790 nm and $R = 0.16$ for 850 nm.

3.4. Multi-distance response of Δ[oxCCO] to functional activation

The response of Δ[oxCCO] to functional activation is shown in Fig. 5 for each detector and separately for each subject. All Δ[oxCCO] responses were statistically significant. A heterogeneous response was found between subjects, with the majority exhibiting an increase in Δ[oxCCO] during functional activation but with some clearly showing a significant decrease. Within the same subject there was good agreement in the directional change of Δ[oxCCO] between detectors.
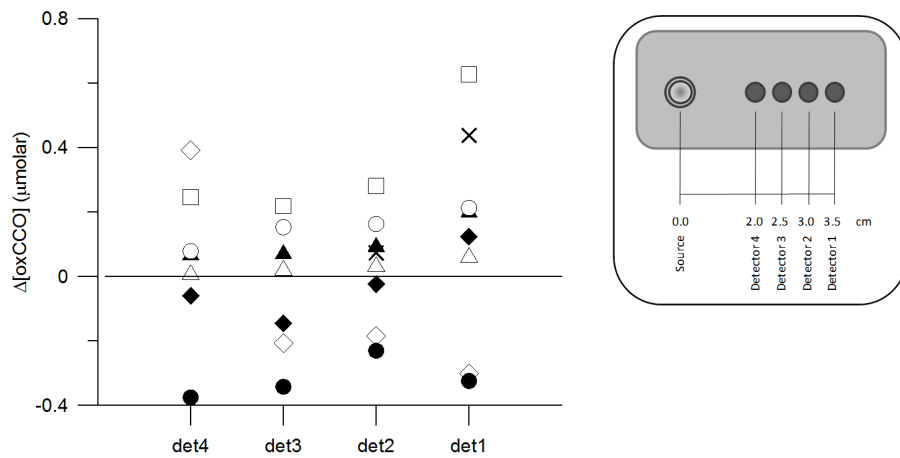

Fig. 5. Response of Δ[oxCCO] between baseline and activation for each of the four detectors. Each symbol corresponds to a different subject, consistent with Fig. 3, 4 and 6. det1-4 denotes detector number, as indicated in the legend. All responses were statistically significant.

Figure 6 shows examples of the individual time-courses of $\Delta[HbO_2]$ and Δ[oxCCO] from two subjects, one case where Δ[oxCCO] increased during functional activation (p<0.0001) and another case where Δ[oxCCO] decreased (p<0.0001). The individual time-courses of Δ[HbO2], Δ[HHb] and Δ[oxCCO] from all subjects are provided in the online supplement, as supplementary Fig. 1.
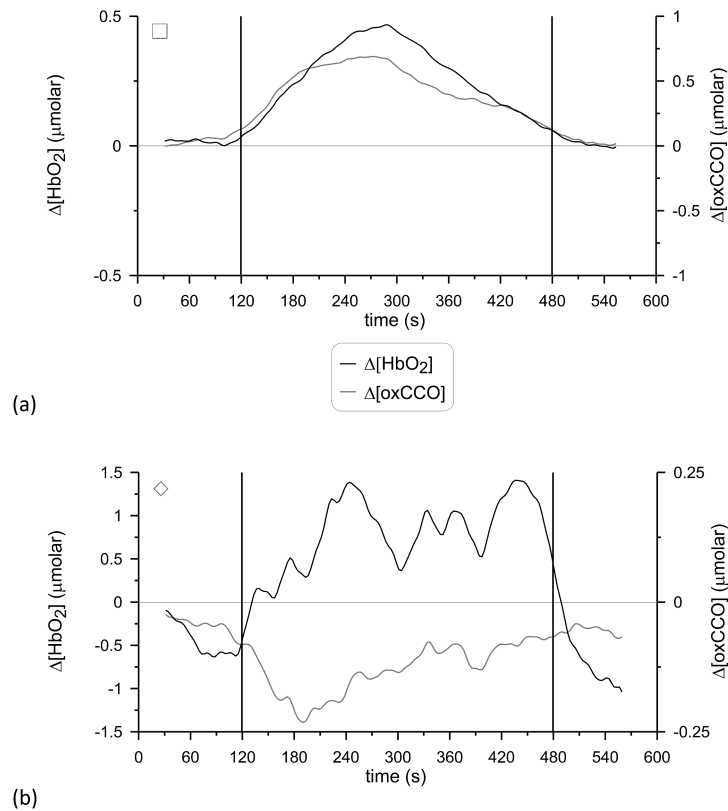
Fig. 6. Examples of the individual time-courses of $\Delta[HbO_2]$ and $\Delta[oxCCO]$ for two subjects. (a): $\Delta[oxCCO]$ increased during functional activation (detector 1) and (b): $\Delta[oxCCO]$ decreased (detector 2). The signals are presented after being filtered with a Butterworth filter and smoothed with a 60-second sliding average window, as described in the Methods. The vertical lines at 120 s and 480 s denote the onset and end of anagram exercise. The symbols at the top left-hand-side corner of each plot indicate the correspondence with Fig. 3, 4 and 5. See Media 2.

4. Discussion

A heterogeneous response of $\Delta[oxCCO]$ to functional activation was measured, with the majority of the participants demonstrating a statistically significant increase in $\Delta[oxCCO]$ during anagram solving and others a statistically significant decrease.

The paradigm of brain functional activation through anagram solving was selected because of its ease of application in an NIRS study and its reliability in inducing functional activation-related changes in the healthy adult brain. Using instrumentation appropriate for CCO redox state measurements, we were able to detect significant changes in $\Delta[oxCCO]$ in all channels that showed a hemodynamic response. The directional change in $\Delta[oxCCO]$ was heterogeneous with some subjects showing an increase and others a decrease (Fig. 5). Thorough analysis was undertaken to ensure that only data sets exhibiting hemodynamic response consistent with functional activation were interrogated for a $\Delta[oxCCO]$ response and to further ensure the step-by-step exclusion of all factors that could have a confounding effect on the CCO redox state measurements. The heterogeneity in the directionality of the $\Delta[oxCCO]$ response therefore appears to be physiological.

Such heterogeneous response of $\Delta[oxCCO]$ (Fig. 5) is not reported in the few existing NIRS functional activation studies investigating CCO [12,14]. Through NIRS measurements

over the occipital lobe, Heekeren et al. showed an increase in the concentration of oxidised CCO during passive visual stimulation (10 s of stimulation followed by 30 s of rest), in the presence of qualitatively similar but quantitatively considerably smaller changes in $\Delta[HbO_2]$ and $\Delta[HHb]$ compared to the present study [14]. Some degree of heterogeneity in the response of $\Delta[oxCCO]$ to functional activation, entirely masked in the group results, was found in the study of Uludağ et al. [12]. The authors implemented an elaborate protocol of passive blob (high CCO content) and interblob (low CCO content) stimulation for the purpose of investigating the influence of haemoglobin cross-talk on the detected $\Delta[oxCCO]$ responses. While not the primary purpose of the study and not commented on by the authors, a significant decrease in the concentration of oxidised CCO was detected in a few individuals, even though on average the concentration of oxidised CCO increased. Since our study and others target different cortical areas and use dissimilar stimulation protocols, a direct comparison is not prudent. Although the $\Delta[oxCCO]$ response in our study is suggestive of a group overall increase in the concentration of oxidised CCO during frontal functional activation (P = NS in all detectors), there is no good reason to believe that the decrease observed in some subjects is not a real physiological response.

Such heterogeneity in the $\Delta[oxCCO]$ response was somewhat surprising, since other studies conducted by our group using broadband spectroscopy in healthy volunteers, and with a similar measuring site and the same algorithms to the present study, detected group significant changes in $\Delta[oxCCO]$ during a variety of protocols inducing global changes in cerebral hemodynamics via manipulation of cerebral oxygen delivery. Tisdall et al. [16] found a significant decrease of 0.24 μmolar (median, P<0.01) in $\Delta[oxCCO]$ during hypoxia (decrease of SaO_2 to 80%). Tachtsidis et al. [17] found a significant increase of 0.09 ± 0.12 μmolar (P<0.05) in $\Delta[oxCCO]$ with hyperoxia (increased inspired oxygen concentration to 100%). During hypercapnia, the same authors found an increase in $\Delta[oxCCO]$ of 0.25 ± 0.17 μmolar (P<0.005). It therefore seems unlikely that the heterogeneous response of $\Delta[oxCCO]$ to functional activation observed in the present study could be induced by factors other than the protocol of functional activation *per se*.

The major contribution to the $\Delta[oxCCO]$ signal is changes in the redox state of the Cu_A centre. The expected response of the redox state of Cu_A to functional activation is not theoretically predictable [8]. An increase in ATP turnover will increase mitochondrial ADP and decrease the magnitude of the mitochondrial membrane potential. When CCO is studied in isolation, given the position of the Cu_A centre in the membrane, dropping the membrane potential causes increase in oxidation as the rate of electron exit from Cu_A is enhanced [36]. However, in the whole mitochondrion or cell, the membrane potential acts on multiple sites of the electron transfer chain simultaneously. It is entirely possible that effects elsewhere could result in an increased reduction rate for Cu_A and therefore cancel out this effect. Indeed, in isolated mitochondria the cytochrome *c* redox state (which is in close redox equilibrium to and hence tracks the Cu_A redox state) can be oxidised or reduced depending on the fine details of the mitochondrial system being studied [37].

The situation is even more complicated in our experimental paradigm as two other factors are affected by functional activation. Oxygen levels can increase due to the increase in blood flow, and NADH levels can increase due to activation of citric acid cycle dehydrogenases. These factors act in opposite ways; increases in NADH can cause an increase in Cu_A reduction, whereas oxygen increases can cause an oxidation [8]. Slight physiological or biochemical differences of an individual may therefore change the direction of the Cu_A response.

Furthermore, mitochondrial redox systems can have significant spatial and temporal variations in their response to stimulation. This is best illustrated with fluorescence measurements of NADH [38]. It has been shown in brain slices that stimulation causes an initial oxidation of NADH followed by a reduction. The strength of the two responses differs depending on the time and region being measured. This has implications for our study. It is

possible that near-infrared light interrogates somewhat different regions of the cortex in different subjects; in this case the difference in spatial sensitivity could explain whether we see an oxidation or a reduction in Cu_A, rather than a fundamental difference in the underlying biochemistry or physiology.

Use of a mathematical model of cerebral circulation and metabolism developed in our group could aid the interpretation of the measured heterogeneous Δ[oxCCO] changes in each individual [9]. The model has been designed for the interpretation of experimental data and can reproduce basic mechanisms of cerebral physiology. Receiving a number of measured variables as input, it is able to generate as output a close likeness of other variables that were not used as input but were measured nonetheless. Most importantly, it is also able to predict variables that cannot be measured, providing an immensely helpful tool in the interpretation of physiological data.

In the light of the heterogeneous response of CCO measured in our study, we used this model to explore the predicted response of CCO to functional activation (modelled as a 30% increase in demand, causing a ~5% increase in CMRO2).

The model allows for the possibility of changing the NAD/NADH ratio via varying the model parameter D_NADH (see supplementary Fig. 2 for details). This represents a change in glycolytic TCA cycle flux during functional activation [39]. Such a change can affect both the magnitude and direction of the Δ[oxCCO] response [9]. Figure 7(a) shows that a relatively small change in the NAD/NADH ratio from 9.0 to 8.1 can change the Δ[oxCCO] response from an oxidation to a reduction; the direction of the Δ[HbO2] and Δ[HHb] responses remains unaffected.

Internal properties of the mitochondrial electron transfer chain, in particular its response to changes in the proton motive force, can also alter the direction of a redox state change following functional activation [8]. To illustrate this we varied the parameter in the model that controls how sensitive the rate of NADH oxidation is to the proton motive force (parameter ck1-see supplementary Fig. 2 for details). Figure 7(b) illustrates how varying this internal parameter can cause a switch in the Δ[oxCCO] response to functional activation, despite only a very modest increase in CMRO2. Again, the direction of the Δ[HbO2] and Δ[HHb] responses remains unaffected.

These examples illustrate that the direction of the Δ[oxCCO] response to functional activation can vary between individuals even if other measured signals appear identical. This confirms that it is not implausible that genuine physiological variations account for the heterogeneous response of Δ[oxCCO] observed in our population. Interestingly, a heterogeneous response of CCO to reperfusion after cerebral ischemia has been used as a discriminator of pathophysiology [40].

Without being the primary finding of the present study, the Δ[HbO$_2$] time to-peak-response that we measured is worthy of comment as it might appear at first glance to be rather long compared to that seen in other functional activation studies. The hemodynamic response to cerebral functional activation is highly variable in terms of time, amplitude and predictability, depending among other factors on the activated area and the task used to activate it [41]. Therefore, in the first instance only comparisons of our study with those involving frontal anagram-evoked stimulation and activation in healthy adults would seem judicious [24,27,28,42–44]. Furthermore, because participants in the present study were subjected to an unusually prolonged task, only studies with similar task duration are considered in the comparison [24,27,28]. In this context, the time to-peak-response found in the present study is of the same order of magnitude as reported in other studies (~1 min), albeit longer.

A tendency for the detectors further away from the source to identify a larger Δ[oxCCO] response, compared to the detectors closer to the source, was present in our data. The furthest detectors have higher depth sensitivity than the closer detectors and therefore interrogate more brain tissue. Because CCO is present in higher concentrations in the brain compared to skin
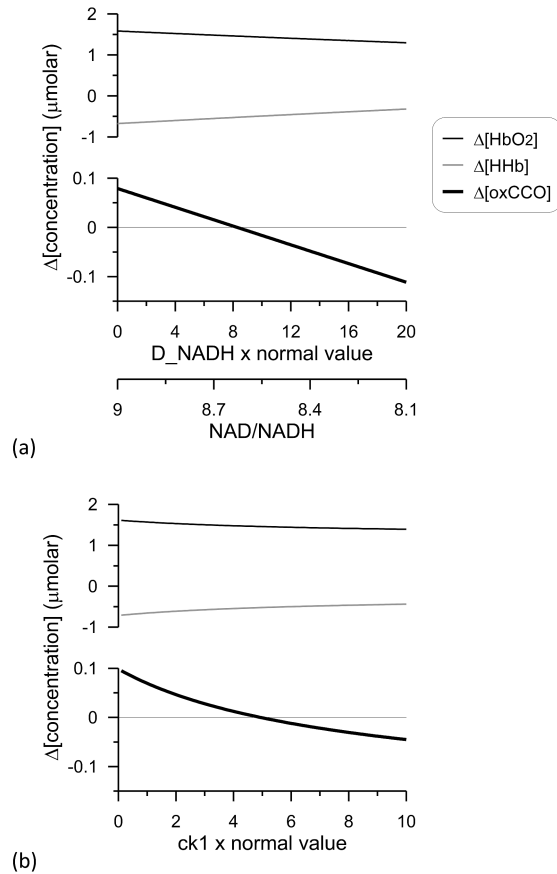
Fig. 7. Modelling of NIRS changes following functional activation. The BRAINSIGNALS model was used [9]. Functional activation was modelled as a 30% increase in demand (parameter change from 1 to 1.3). (a): Model parameter D_NADH was varied with respect to its normal value in the model and the accompanying optical changes and NAD/NADH ratios plotted. (b): Model parameter ck1 was varied with respect to its normal value in the model and the accompanying optical changes plotted. See Media 3.

[45], such incremental Δ[oxCCO] response with increasing source-detector separation is to be expected.

In cerebral functional activation studies, concerns about simultaneous task-evoked changes in scalp hemodynamics interfering with and obscuring the NIRS signals from the deeper layers are common [23–25,27,28]. Although hemodynamic fluctuations in the scalp due to task-induced changes in heart rate and blood pressure introduce physiological noise in the NIRS signals, changes in scalp perfusion are difficult to unravel from the actual changes in cerebral perfusion. It can be anticipated that the degree of scalp contamination introduced in the NIRS signals would strongly depend on whether or not the optodes were placed directly over large scalp vessels, but this information cannot be retrieved retrospectively in the present study. However, with respect to Δ[oxCCO] (the primary target of this study), the absence of significant correlations with the measured systemic variables in terms of amplitude of response indicates that the observed changes in oxidised CCO concentration are not the effect of interference from the superficial layers. In any case, the Δ[oxCCO] signal is expected to be less prone to extracerebral contamination, since CCO is present only in small concentrations in the scalp [46].

An experimental study by Schytz et al. [47] suggested that NIRS data obtained with a multi-distance source-detector configuration can be decontaminated from the effect of skin blood flow by using the short source-detector separation measurements (1 cm) to correct the long source-detector separation measurements (3 cm). The shortest source-detector separation in the pHOS is however 2 cm, a distance long enough for the detector to pick up some brain signal [48,49], and therefore using these measurements to decontaminate the 3.0 and 3.5 cm measurements would produce erroneous results. It is also acknowledged that Monte Carlo simulations in the adult head suggest an error of over 20% in the measurement of optical absorption using an FD spectrometer with source-detector spacing between 3.0 and 4.5 cm, induced by the extra-cerebral tissue [50]. From the practical point of view, we attempted to reduce the interference from the superficial layers by firm application of the optodes on the forehead and using mostly the recordings from the distal detector to draw conclusions about the behaviour of CCO during functional activation. The lack of correlations between Δ[oxCCO] and systemic variables indicates that this approach was sufficient.

Experimental considerations: We are aware of concerns regarding the depth sensitivity of NIRS, however we believe that in our study the tissue volume interrogated by the FD and broadband components could not have been substantially different. Firstly, because in terms of detector positioning within each pHOS optode, the two long source-detector separations (3.0 and 3.5 cm) of the FD and broadband components were equivalent. Secondly, because for the adult human head the difference in the interrogated tissue volume due to different wavelengths of near-infrared light is very small [51]. Regardless, even if there was some difference in the interrogated tissue volume between the two modalities, it could not have selectively distorted our findings. Both Δ[oxCCO] and Δ[HbO$_2$] concentrations were calculated using exactly the same method; the haemoglobin measurements showed a response consistent with functional activation and in the presence of this response, we investigated the corresponding Δ[oxCCO] response.

It is obvious from Fig. 5 that two subjects showed a heterogeneous response of Δ[oxCCO] to functional activation between different detectors. We cannot exclude the possibility that, in the same subject, due to the different depth sensitivity of the detectors, the different interrogated regions exhibited different Δ[oxCCO] response to functional activation. We consider this finding to be an advocate against averaging data from different detectors.

DPF was calculated from μ_a and μ_s' based on a relationship derived from the diffusion theory assuming a semi-infinite turbid medium [31]. It is possible that differences between the geometry of this model and the adult head will induce further errors in the calculation of DPF.

An effect of haemoglobin cross-talk was not evident in our data. Spectroscopic cross-talk can arise from the wavelength dependency of the partial photon pathlength of the activated cortical volume and is demonstrated as a change in one chromophore mimicking the change in another [11,12]. Although we investigated the effect of functional activation on Δ[oxCCO] only in the presence of a concomitant increase in Δ[HbO$_2$], the directionality of the Δ[oxCCO] response was not homogenous, as would be expected if it was solely the result of cross-talk from the (homogenous) Δ[HbO$_2$] response. Furthermore, linear regression analysis revealed no statistically significant correlations between the response of Δ[oxCCO] and Δ[HbO$_2$] or between the response of Δ[oxCCO] and Δ[HbT] = Δ[HbO$_2$] + Δ[HHb], with an average R-value over all detectors of R = 0.21 for Δ[HbO$_2$] and R = 0.16 for Δ[HbT].

In future studies, the option to induce frontal lobe functional activation with a less prolonged task, which could be repeated several times for each subject, should be considered for the purpose of investigating the homogeneity of the directional changes in Δ[oxCCO] within subjects. Finally, the possibility that the prolonged stimulation protocol led to habituation effects in the present study cannot be excluded.

5. Conclusion

A heterogeneous response of Δ[oxCCO] to functional activation was found, with most subjects exhibiting an increase in Δ[oxCCO] during anagram solving, but with some showing a decrease. We suggest that this heterogeneity has a physiological interpretation and is not induced by confounding factors in the measurements.

Acknowledgments